Single Molecule Electrochemistry

Fu-Ren F. Fan,[†] Juhyoun Kwak,[‡] and Allen J. Bard*[,†]

Contribution from the Department of Chemistry and Biochemistry, The University of Texas at Austin, Austin, Texas 78712, and Department of Chemistry, Korea Advanced Institute of Science and Technology, Taejon, Korea 305-701

Received April 2, 1996[⊗]

Abstract: By using specially constructed nanometer tips of sharpened Pt-Ir wire in a wax sheath, small numbers of molecules (1−10) can be trapped between the tip and a substrate. Repeated electron transfers of an electroactive molecule as it shuttles by diffusion between tip and substrate produce a current (∼0.6 pA/molecule) that can be used to detect the trapped molecules. The tip electrode size and shape can be found from the electrode approach curves (current vs tip-to-substrate distance) based on approximate equations and digital simulations. Analysis of the observed fluctuating currents by autocorrelation, spectral density, and probability density functions is also described.

Introduction

We report here electrochemical studies at the level of single molecules and small numbers of molecules. The detection of single molecules, their characterization, and their chemical and physical manipulation have come within current scientific capability and have become topics of significant interest. Electrochemical measurements on single molecules should allow determination of standard half-reaction potentials and free energies, diffusion coefficients, and kinetic parameters. To our knowledge the work reported here represents the first example of controlled redox chemistry at the single molecule level. Electroanalytical chemistry at this level represents the ultimate sensitivity in trace chemical analysis, and such studies are being undertaken with the expectation that investigations of properties and reactions at the single molecule level will allow one to discover effects, e.g., of molecular environment, that cannot be observed because they are averaged out when one makes measurements on a large number of molecules. A number of techniques have been used in recent years to detect single molecules or ions in different environments. These include the detection of ions that are confined in a vacuum in electromagnetic traps,[1] single-molecule spectroscopy of molecules in solid matrices,[2] the detection of individual dye molecules in solution by far-field confocal fluorescence microscopy,[3] and the detection of molecules on surfaces with high spatial resolution by near-field scanning optical microscopy.[4−8] Single-molecule detection (SMD) has also been achieved for molecules spatially restricted in microdroplets[9] and in a thin flow cell.[10] Recently, Collinson and Wightman[11] observed individual chemical reactions in solution by detecting temporally resolved electrogenerated chemiluminescence at an ultramicroelectrode with a multichannel scaler.

In a recent communication,[12] we reported SMD for an electroactive molecule in solution as it repeatedly undergoes electron-transfer reactions at an electrode held at a small distance from a substrate in a scanning electrochemical microscope (SECM). Briefly, the current at a small Pt disk electrode (radius ∼10−20 nm) encased and slightly recessed in a wax sheath is measured as it is moved toward a conductive substrate in a solution containing an electroactive species and excess inert supporting electrolyte. The tip contacts the substrate and traps one or more molecules in the gap between disk and substrate. The electroactive molecules diffuse back and forth between the disk electrode and substrate undergoing redox processes at each, thus producing a current flow (Figure 1A). In this report we describe further electrochemical SMD experiments focussing on the SECM characterization of the cell geometry, the effect of substrate conductance on the tip current fluctuation at various distances, and statistical analyses of the response based on the time correlation, power spectral density, and probability density functions.

Experimental Section

Materials. Unless otherwise mentioned, in all of the experiments, [(trimethylammonio)methyl]ferrocene (CP_2FeTMA^+)[13] was used as the electroactive molecule. This species was selected because both it and its oxidized product are stable in aqueous media and undergo rapid heterogeneous electron-transfer reactions at electrodes in a convenient range of potentials. Both indium tin oxide (ITO) on glass (Delta Technologies, Inc., Stillwater, MN) and a 1-mm-thick, (001)-oriented n-TiO_2 single-crystal sample (Fuji Titan, ca. 5 mm × 5 mm) were used as the substrates. ITO was degreased in trichloroethylene (Aldrich, Milwaukee, WI) and was subsequently washed with ethanol and dried in air before use. The n-TiO_2 (001) single-crystal sample was polished, finished, cleaned, and reduced according to previously reported

[†] University of Texas.
[‡] KAIST.
[⊗] Abstract published in *Advance ACS Abstracts,* September 15, 1996.

(1) See, for example, Itano, W. M.; Bergquist, J. C.; Wineland, D. J. *Science* **1987**, *237*, 612.
(2) Moerner, W. E. *Science* **1994**, *265*, 46.
(3) Nie, S.; Chiu, D. T.; Zare, R. N. *Science* **1994**, *266*, 1018.
(4) Betzig, E.; Trautman, J. K.; Harris, T. D. Weiner, J. S.; Kostelak, R. L. *Science* **1991**, *251*, 1468.
(5) Betzig, E; Chichester, R. J. *Science* **1993**, *262*, 1422.
(6) Xie, X. S.; Dunn, R. C. *Science* **1994**, *265*, 361.
(7) Ambrose, W. P.; Goodwin, P. M.; Martin, J. C.; Keller, R. A. *Phys. Rev. Lett.* B **1994**, *72*, 160.
(8) Trautman, J. K.; Macklin, J. J.; Brus, L. E.; Betzig, E. *Nature* **1994**, *369*, 40.
(9) Barnes, M. D.; Ng, K. C.; Whitten, W. B.; Ramsey, J. M. *Anal. Chem.* **1993**, *65*, 2360.
(10) Dovichi, N. J.; Martin, J. C.; Jett, J. H.; Keller, R. A. *Science* **1982**, *219*, 845.
(11) Collinson, M. M.; Wightman, R. M. *Science* **1995**, *268*, 1883.
(12) Fan, F.-R., Bard, A. J. *Science* **1995**, *267*, 871.
(13) Henning, T. P.; White, H. S.; Bard, A. J. *J. Am. Chem. Soc.* **1981**, *103*, 3937.

S0002-7863(96)01079-7 CCC: $12.00

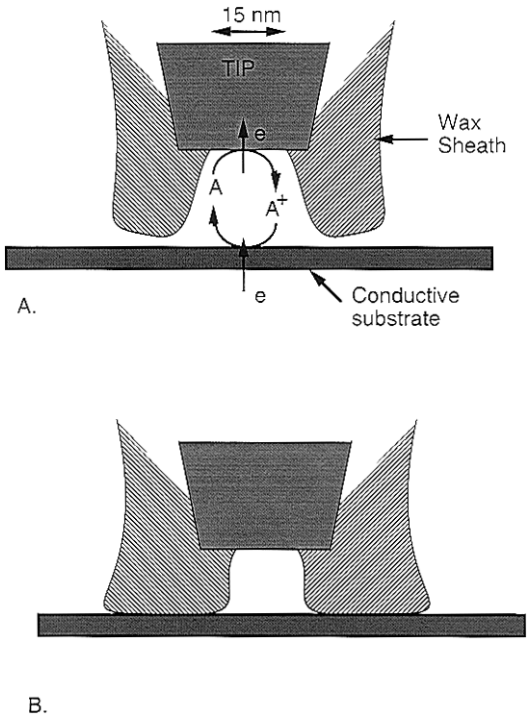

Figure 1. (A) Idealized diagram of the trapping of molecule A that is oxidized at the tip electrode. The product A^+ is reduced at the substrate. (B) Schematic diagram of the effect of compressing wax tip coating against substrate.

procedures.[14] A layer of In-Ga alloy was then plated onto the backside of the sample to serve as an ohmic contact, which was connected to a thin platinum wire. The entire crystal (except its front surface) including the ohmic contact and part of the connecting wire was then electrically shielded with (Miccro Super XP2000) stop-off lacquer (Tolber Division, Michigan Chrome and Chemical Company, Hope, AR). A 1 M $NaNO_3$ solution was used as the supporting electrolyte. All other chemicals were reagent grade and were used without further purification. Millipore reagent water (> 18 MΩ) was used for the preparation of aqueous solutions. Pt-Ir (80%-20%) wire (0.250-mm diameter), used to construct tips, was obtained from FHC Co. (Brunswick, ME).

Tip Preparation and Apparatus. The ultramicrotips used in this experiment were prepared by the procedures described previously.[15] Insulation of the tip was done with Apiezon wax or polyethylene glue following the procedure reported by Nagahara et al.[16] The insulated tip was then mounted on the SECM in a cell containing a redox electrolyte (e.g., 2 mM Cp_2FeTMA^+ in 1.0 M $NaNO_3$). The success of the tip insulation procedure was checked by cyclic voltammetry in this solution. For a well-insulated tip, the tip current during an initial scan, i_T, was less than 50 fA. The very end of the tip was then exposed in the SECM by the following procedure. The potentials of the tip and a conductive substrate (e.g., ITO) were biased at suitable values (e.g., 0.60 V vs a saturated calomel electrode (SCE) for the tip and −0.20 V for the substrate) with the SECM operated in the constant current mode (e.g., with a reference current of 10 pA). As the well-insulated tip approached the surface of the substrate, the onset of an enhanced current flow caused the z-piezo to retract the tip. This process produced a hole in the tip insulation at the point of closest approach of tip to substrate, while leaving most of the tip still insulated. The exposed area of the tip could be estimated from the steady-state tip current with the tip far away from the substrate, $i_{T,\infty}$. The basic instrument used in this experiment has been described previously[17] and is capable of both STM and SECM measurements with a current sensitivity as low as 50 fA. The electrochemical cell contained a Pt counter electrode and either an SCE or a Pt quasi-reference electrode (PtQRE) as a reference electrode.

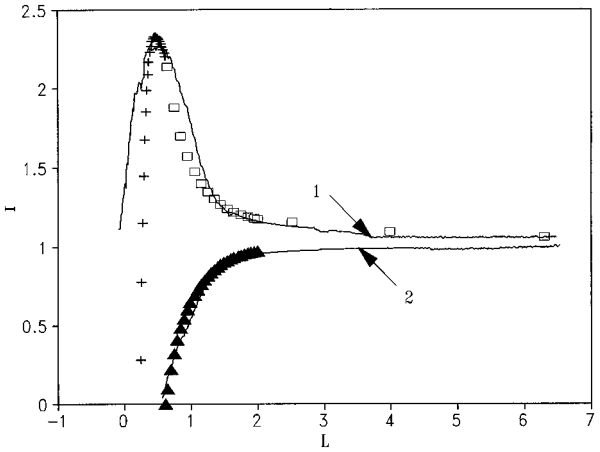

Figure 2. Dependence of tip current (normalized to $i_{T,\infty}$) on relative tip displacement (normalized to tip radius) over a conductive n-TiO_2 substrate ($E_S = -0.7$ V vs SCE), curve 1, and an insulating n-TiO_2 substrate ($E_S = 0.0$ V vs SCE), curve 2, in a solution containing 2 mM Cp_2FeTMA^+ and 1.0 M $NaNO_3$. The tip was biased at 0.60 V vs SCE. The tip moved to the substrate surface at a rate of 38 Å/s. Solid curves are experimental data and symbols are theory. (□) Simulated data for conducting substrate; (+) calculated data based on eq 3; (Δ) simulated data for insulating substrate. Fitting parameters: $a = 45$ nm, $a_0 = 67$ nm, $l = 28$ nm, and $D = 5.0 \times 10^{-6}$ cm²/s. Experimental $i_{T,\infty}$ is equal to 9.0 pA.

Results and Discussion

The results described below are representative of the large number of experiments that were carried out. A chronology of the experiments and additional results and figures (Figures S1−S9) showing related experiments are given in the supporting information.

Tip Current vs Distance. The SMD experiment requires a tip of small diameter that is slightly recessed within the wax sheath. While it is not possible to remove the tip after preparation from the SECM cell and examine it by electron microscopy, information about the exposed area of the tip and the shapes of the tip and insulating sheath can be obtained from electrochemical measurements, that is, from SECM approach curves where the tip current, i_T, is measured as a function of tip-substrate spacing, d, as the tip is moved toward the substrate.[18] Tips with the correct configuration show approach curves like those in Figure 2; these were obtained with a solution containing 2 mM Cp_2FeTMA^+ and 1.0 M $NaNO_3$, with the tip biased at 0.6 V vs SCE (where Cp_2FeTMA^+ oxidation is diffusion-controlled). In the experiment in Figure 2 (curve 1), the n-TiO_2 substrate was biased at −0.7 V vs SCE, so that Cp_2FeTMA^{2+} generated at the tip was rapidly reduced back to Cp_2FeTMA^+ at the n-TiO_2 surface. A similar approach curve has previously been reported for the same solution and ITO substrate.[12] Since n-TiO_2 is a semiconductor, when it is biased at a potential negative of its flat-band potential ($V_{fb} \approx -0.25$ V vs SCE in this solution), it is forward-biased and is electronically conductive. When it is reverse-biased or biased at a potential positive of V_{fb} (e.g., 0 V vs SCE), the n-TiO_2 surface becomes insulating.[19] Hence, experiments can be carried out with the

(14) Fan, F.-R., Bard, A. J. *J. Phys. Chem.* **1990**, *94*, 3761 and references therein.

(15) Fan, F.-R., Mirkin, M. V.; Bard, A. J. *J. Phys. Chem.* **1994**, *98*, 1475.

(16) Nagahara, L. A.; Thundat, T.; Lindsay, S. M. *Rev. Sci. Instrum.* **1989**, *60*, 3128.

(17) Fan, F.-R., Bard, A. J. *J. Electrochem. Soc.* **1989**, *136*, 3216.

(18) Mirkin, M. V.; Fan, F.-R.; Bard, A. J. *J. Electroanal. Chem.* **1992**, *328*, 47.

(19) See, for example: *Semiconductor Electrodes*; Finklea, H. O., Ed.; Elsevier: Amsterdam, 1988.

Scheme 1

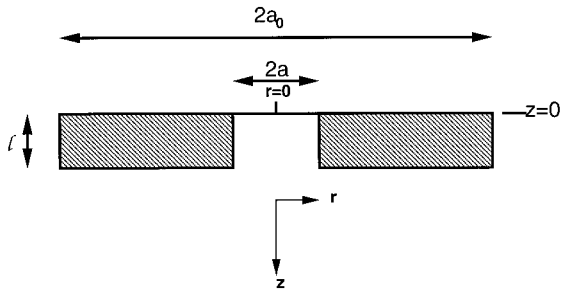

Table 1. Normalized Tip Current for a Recessed Disk Electrode

$L = l/a$	$I_T = i_{T,\infty}/4nFDC^b a$	$L = l/a$	$I_T = i_{T,\infty}/4nFDC^b a$
0.00	1.000 00	1.20	0.382 19
0.20	0.762 82	1.40	0.347 86
0.40	0.633 94	1.60	0.319 21
0.60	0.543 79	1.80	0.294 95
0.80	0.476 46	2.00	0.274 12
1.00	0.424 11		

same tip and solution without making any changes, while the conductance of an n-TiO_2 substrate is controlled by adjusting its bias potential. Additional experiments of this type are shown in Figures S2, S3, and S7.

The exposed radius a of a normal disk-shaped electrode can be determined from the steady-state current, $i^0_{T,\infty}$, when it is far away from the substrate from the equation[20]

$$i^0_{T,\infty} = 4nFDC^b a \quad (1)$$

where n is the number of electrons involved in the redox reaction (1 for Cp_2FeTMA^+), F is the Faraday constant, D is the diffusion coefficient, and C^b is the bulk concentration of Cp_2FeTMA^+. However, as discussed below, the tip produced by the procedure described here is recessed slightly within the insulating wax sheath. Such a recessed disk electrode produces a different response.[21] For a recessed disk-shaped electrode with the geometry shown in Scheme 1, $i_{T,\infty}$ is given by an approximate equation (see Appendix A)

$$i_{T,\infty} = [\pi a/(4l + \pi a)]i^0_{T,\infty} \quad (2)$$

where l is the recessed depth of the disk electrode. $i_{T,\infty}$ can also be obtained by digital simulation (Appendix B) as a function of $L = l/a$ (Table 1). For the normalized tip current ($I_T = i_{T,\infty}/i^0_{T,\infty}$), the difference between the value calculated by the approximate analytical equation (eq 2) and the simulated value is less than 3.4%, when $l > 0.2a$.

The approach curve shape also depends on tip shape. For a coplanar disk, i_T increases monotonically with decreasing d for a conductive substrate and diffusion-controlled reactions at tip and substrate.[20] For a recessed disk, the SECM positive-feedback process starts to become significant when the tip approaches a conductive n-TiO_2 substrate ($E_S = -0.7$ V vs SCE) to within a few tip diameters (Figure 2, curve 1). The agreement between experimental and simulated data (Appendix B) (for $l = 0.62a$, $a = 45$ nm) is reasonably good up to a distance d about equal to the recessed depth l, at which point the insulating sheath starts to compress against the substrate. However, different from a normal disk electrode (i.e., one with $l = 0$), which shows a monotonically increasing tip current, with tips constructed as described above, the tip current increases to reach a maximum and then decreases as the tip comes even closer before showing a large increase (not shown) presumably because of the occurrence of electron tunneling between tip and substrate. Although this current decrease might be attributed to heterogeneous kinetic effects on the electron-transfer reactions,[22] this behavior was found at even more extreme tip or substrate potentials for various substrates and other redox couples. We thus believe that this region of current behavior is related to the deformation of the insulating sheath as it is pressed against the substrate at very small distances (as shown in Figure 1B). Consider an idealized thin-layer cell as shown in Scheme 2, where we assume that the insulating wax flows inward and outward by equal amounts as it is compressed against the substrate. When this occurs, the steady-state current of the thin-layer cell confined by the disk, substrate, and insulating sheath is given by the following equation (see Appendix C).

Scheme 2

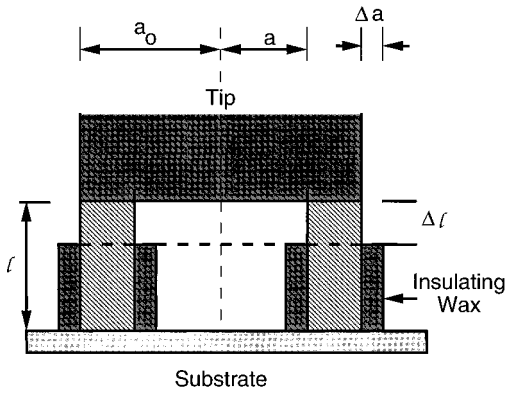

$$i_{TLC} = \{\pi[2la^2 - \Delta l(a_0^2 + a^2)]/[8a(l - \Delta l)^2]\}i^0_{T,\infty} \quad (3)$$

where $i^0_{T,\infty}$ is given by eq 1, a is the initial disk radius, a_0 is the initial outer radius of the insulating sheath before the compression occurs, and Δl is the change of the recessed depth of the disk electrode during compression. As implied in eq 3, if $a_0 < \sqrt{3}a$, the tip current will increase to reach a maximum at Δl equal to $l(3a^2 - a_0^2)/(a_0^2 + a^2)$ and then decrease as the tip comes even closer to the surface of the substrate; otherwise, it will reach the maximum at $\Delta l = 0$. As shown in Figure 2, curve 1, there is some discrepancy between the experimental curve and the theoretically calculated data based on eq 3, perhaps because Δl is not exactly equal to the nominal tip displacement due to the finite compressibility of the insulating wax and deviations from the assumed idealized model. With a diffusion coefficient of Cp_2FeTMA^+ of 5×10^{-6} cm^2/s, the theoretical fit of the experimental approach curve yields $a = 45$ nm, $a_0 = 67$ nm, and $l = 28$ nm.

When the n-TiO_2 substrate is in its insulating state (e.g., $E_S = 0$ V vs SCE), the approach curve is that shown in Figure 2, curve 2. Here the behavior of the recessed tip is similar to that of a usual disk electrode and decreases monotonically with decreasing distance.

Fluctuation of the Tip Current at Small Distances. The Effect of Substrate Conductance. The previous study of tip current fluctuations at small distances where a small number of electroactive molecules were trapped between tip and substrate focussed on a conductive substrate.[12] Here we compare the fluctuation behavior of tip current on both

(20) Bard, A. J.; Fan, F.-R.; Mirkin, M. V. In *Electroanalytical Chemistry*; Bard, A. J., Ed.; Marcel Dekker: New York, 1994; Vol. 18, pp 243−373.

(21) (a) Baranski, A. S. *J. Electroanal. Chem.* **1991**, *307*, 287. (b) Oldham, K. B. *Anal. Chem.* **1992**, *64*, 646. (c) Scott, E. R.; White, H. S.; Phipps, J. B. *J. Membrane Sci.* **1991**, *58*, 71.

(22) Mirkin, M. V.; Bard, A. J. *J. Electroanal. Chem.* **1992**, *323*, 1.

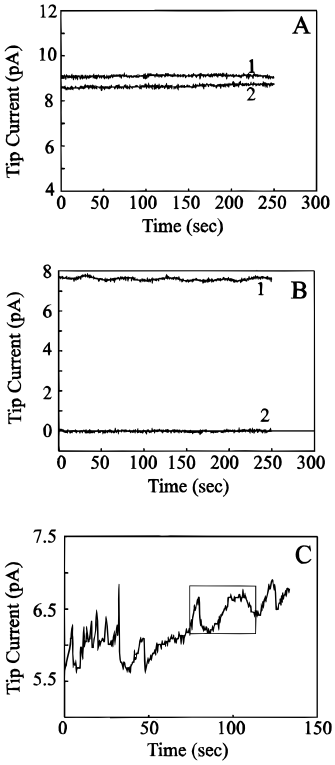

Figure 3. Time evolution of the tip current observed at a tip potential $E_T = 0.6$ V and a n-TiO_2 substrate potential $E_S = -0.7$ V (curve 1) or 0.0 V (curve 2) vs SCE for various distances in a solution containing 2 mM Cp_2FeTMA^+ and 1.0 M $NaNO_3$. The data sampling rate was 0.4 s per point. (A) With tip far away from the substrate; (B) $d \approx 13$ nm, which gave an average steady-state tip current of ~7.6 pA when $E_S = -0.7$ V vs SCE; (C) $d \approx 11$ nm, which gave an average steady-state tip current of ~6.1 pA.

conductive and insulating substrates. As found in the previous studies, the fluctuation intensity was strongly dependent on the distance. To ensure that we were measuring two different fluctuation behaviors at the same distance, we used the same substrate, n-TiO_2, held at a fixed distance and changed its conductance simply by varying its bias potential. As shown in Figure 3A, when the tip was far away from the substrate (e.g., $d/a > 2$), only a very small fluctuation in the tip current was observed when the substrate was either conductive ($E_S = -0.7$ V vs SCE) or insulating ($E_S = 0.0$ V vs SCE). As expected at such a distance, the current was slightly higher when the substrate was conductive than when it was insulating. When the tip approached to within the recessed depth of the disk electrode (i.e., $d < l$), considerable fluctuation in the tip current was observed when the substrate was conductive, while i_T was essentially zero and its fluctuation was negligibly small when the substrate was insulating (see Figure 3B). This suggests that the positive feedback of the SECM is responsible for the high amplification of the tip current, which allows for very high detection sensitivity of only a few molecules of electroactive species. When the tip was moved even closer to the surface of the substrate, the tip current decreased because of the decrease of the active area of the electrode (as discussed in the previous section), but the relative fluctuation of i_T intensified (see Figure 3C).

Data Analysis. Exact mathematical descriptions of the data shown in Figure 3C are not possible in the absence of a better understanding of the processes causing the larger current fluctuations and the microscopically detailed cell geometry. However, we can analyze the results by taking the data to be nondeterministic or random. In cases where no explicit

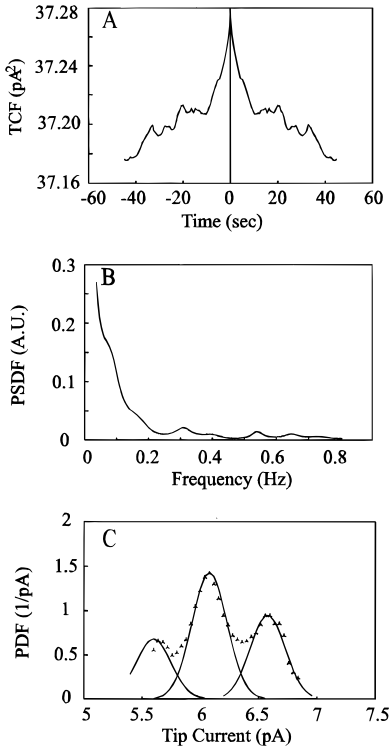

Figure 4. (A) Time correlation function, (B) power spectral density function, and (C) probability density function of the time series in Figure 3.

mathematical equation can be written for the time histories produced by a random phenomenon, statistical procedures are usually used to define the descriptive properties of the data.[23,24] Three of the basic statistical properties for describing random data, i.e., the autocorrelation function, the spectral density function, and the probability density function, for the time series in Figure 3C are shown in Figure 4. The autocorrelation function for a time history record $x(t)$, or the time correlation function (TCF), is a measure of time-related properties in the data that are separated by fixed time delays and is defined as[23,24]

$$\mathrm{TCF}(\tau) \equiv \lim_{T\to\infty} \frac{1}{T}\int_0^T x(t)x(t+\tau)dt \qquad (4)$$

in which τ is the time delay and T is the available record length or some desired portion of the record length. The power spectral density function, PSDF, of $x(t)$ is related to the TCF through Fourier transformation and is given by[23]

$$\mathrm{PSDF}(f) = 4\int_0^\infty \mathrm{TCF}(\tau)\cos(2\pi f\tau)d\tau \qquad (5)$$

in which f is the frequency. Both TCF and PSDF provide information on the rate of fluctuation in a time history record. As shown in Figure 4A, the coherence of the data is high, and TCF indicates that several fluctuation processes occur at frequencies on the order of a few tenths of a hertz. Parallel to the TCF, the PSDF of the time series is fairly broad and contains several peaks at frequencies on the order of fractions of hertz (Figure 4B). From the autocorrelation of the time series at zero and infinite time displacements, a mean square tip current of 37.3 $(pA)^2$ and a mean tip current of 6.1 pA can be obtained,

(23) Bendat, J. S.; Piersol, A. G. *Random Data Analysis and Measurement Procedures*, 2nd ed.; J. Wiley and Sons: New York, 1986.
(24) Van Kampen, N. G. *Stochastic Processes in Physics and Chemistry;* North Holland: Amsterdam, 1992.

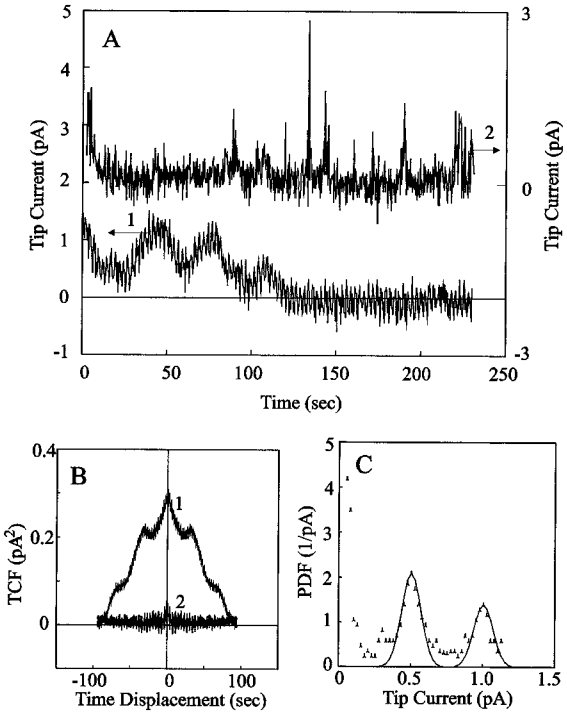

Figure 5. (A) Time history record of the tip current observed at a tip potential of 0.55 V and an ITO substrate potential of −0.3 V vs SCE. $a \approx 7$ nm. Curve 1: $d \approx 10$ nm, solution: 2 mM Cp_2FeTMA^+ and 2.0 M $NaNO_3$. Curve 2: d was within tunneling range in a solution containing only 2.0 M $NaNO_3$. The data sampling rate was 0.4 s per point. (B) Time correlation function and (C) probability density function of the time series A, curve 1.

respectively. A mean tip current of 6.1 pA is consistent with the estimate from Figure 3C, which shows that the tip current fluctuates around 6 pA with a fluctuating amplitude of about 0.5 pA. A more accurate analysis is based on the probability density function (PDF), which describes the probability that the data will assume a value within some defined range at any instant of time. In equation form, it is defined as follows:[23]

$$\mathrm{PDF} = \lim_{\Delta x \to \infty} \frac{\mathrm{Prob}[x < x(t) < x + \Delta x]}{\Delta x} = \lim_{\Delta x \to 0}\left[\lim_{T \to \infty} \frac{Tx}{T}\right] \tag{6}$$

in which Prob[$x < x(t) < x + \Delta x$] is the probability that $x(t)$ assumes a value within the range between x and $(x + \Delta x)$, and Tx is the total amount of time that $x(t)$ falls inside the range (x, $x + \Delta x$) during an observation time T. As shown in Figure 4C, the PDF of the time series of Figure 3C contains several Gaussian peaks. The most probable tip currents are spaced 0.5 pA apart, with a standard deviation of the peaks of ∼0.1 pA.

We have also applied statistical methods to analyze the tip current time series observed on a different conductive substrate, indium tin oxide (ITO). Figure 5A shows a tip current time series observed on ITO that we reported previously.[12] This series was obtained using a tip with a much smaller radius ($a \approx 7$ nm) than was used in Figure 3. So the average tip current was much smaller than that shown in Figure 3C for a comparable tip-substrate spacing and the same concentration of electroactive species; however, a similar flucuation amplitude in the tip current was observed in both cases. The TCF of the series in Figure 5A also shows that multiple fluctuation processes with fluctuating frequencies in the range of fractions of hertz are involved (Figure 5B). The multiple bell-shaped probability density plot shown in Figure 5C again is characterized by a stepwise transition character of the fluctuation of the tip current. Thus, the fluctuation pattern of the tip current is apparently not strongly dependent on the substrate if the heterogeneous electron-transfer kinetics on the substrate under the experimental condition are rapid.

The TLC equation, eq 7, can be used to calculate, N, the average number of Cp_2FeTMA^+ molecules trapped in a cylindrical TLC with a base radius of 15 nm and height equal to 11 nm, which will produce a limiting steady-state current of 6.1 pA for $D = 5 \times 10^{-6}$ cm²/s.

$$i_{\mathrm{TLC}} = nFADC^{\mathrm{b}}/d = nF\pi a^2 DC^{\mathrm{b}}/d \tag{7}$$

For the cylindrical geometry,

$$i_{\mathrm{TLC}} = nFDN/d^2 N_{\mathrm{AV}} \tag{8}$$

where N_{AV} is Avogadro's number. From eq 8 with $n = 1$ and the conditions given above, N is about 10. Thus, each molecule contributes 0.6 pA of current. Note that the TLC in eq 8 is equivalent to the expression derived from the average transit time between tip and substrate, t_{d},

$$t_{\mathrm{d}} = d^2/2D \tag{9}$$

$$i = nNe/2t_{\mathrm{d}} = nNeD/d^2 \tag{10}$$

where e is the electronic charge ($e = F/N_{\mathrm{AV}}$). The factor of 2 in eq 10 accounts for the fact that it takes twice the time, t_{d}, for one electron-transfer event to occur at the tip. Taking $N = 1$, $D = 5 \times 10^{-6}$ cm²/s, and $d = 11$ nm, a tip current of ∼0.6 pA is obtained. Note that the fluctuation amplitude of the tip current around the mean value as shown in Figure 3C is 0.6 pA.

An exact mathematical description of the entire time series of the tip current based on a deterministic model is not possible. Not only does it require sufficient knowledge of the basic mechanisms of the fluctuation phenomena, which are still not clear, but also it involves inherently stochastic processes involving movement of molecules into and out of the tip/substrate chamber, thermal fluctuations, and other random processes. However, a limited description of the general shape of the current fluctuation is of interest. Assuming that the redox molecules diffuse inside the TLC with a constant D, as suggested by eq 10, there are at least two possibilities which might cause the tip current to change with time: (1) changes in d and the electrode area, for example, because of temperature fluctuations and (2) fluctuations in the number of molecules, N. A continuous change in d without changing N cannot cause a stepwise fluctuation in the tip current; however, it might account for a slow drift of the TLC current. The probability of large step or quantized changes in d without changing N is small. We cannot rule out the possibility that the electric field in the gap may also affect the observed behavior, especially at very small supporting electrolyte concentrations.[25,26] In the work described here, however, a high concentration of supporting electrolyte was employed. Further work will be required to explore possible electric field effects.

The experimental shapes of the rise and fall of the current can be fit very approximately (Figure 6) by an exponential rise and fall with time constants of the order of 2−10 s (attributed to thermal variations in d), a residence time (time for the current to rise and fall) of 5−15 s, and a time between events of the

(25) Fan, F.-R., Bard, A. J., unpublished data.
(26) Smith, C. P.; White, H. S. *Anal. Chem.* **1993**, *65*, 3343.

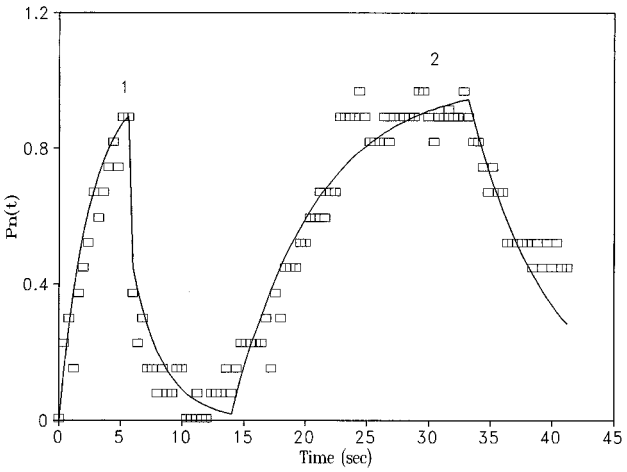

Figure 6. Curve fitting of the marked portion of the time series shown in Figure 3C based on exponential deviate and with fitting parameters. Rising time constant = 2.5 s, rising period = 5.6 s, and falling period = 10 s for peak 1, and rising time constant = 6.7 s and rising period = 16.4 s for peak 2. Symbols are experimental data and solid curve is theory.

order of 10 s, for the conditions of this experiment. These results are consistent with the TCF and PSDF analyses shown in Figure 4.

Conclusions

This study has shown that the positive feedback of the SECM is responsible for the observation of significant fluctuations in the tip current. Both TCF and PSDF analyses indicate that multiple fluctuation processes with the frequencies of fluctuation on the order of a few tenths of a hertz. The PDF contains several bell-shaped Gaussian peaks. The most probable tip currents at the given cell parameters (base radius = 15 nm and height = 11.2 nm) and C^b equal to 2 mM are spaced 0.5 (±0.1) pA apart. These fluctuation amplitudes of the current time series correspond quite well with the contribution current expected for a single molecule in a TLC of that geometry. Very similar fluctuation behavior of the tip currents was observed for both ITO and n-TiO_2 in the conductive state.

Appendix A

Approximate Equation for Recessed Electrode. An equation for the recessed ultramicrodisk can be obtained by assuming that the small recessed layer behaves as a thin layer cell (TLC) bounded by the disk and the bulk solution. The concentration gradient at steady state at the surface of the usual disk electrode coplanar with its insulating sheath with the following boundary conditions

$$C = 0 \quad z = 0 \quad r \le a$$

$$\partial C/\partial z = 0 \quad z = 0 \quad r > a$$

$$C = C^b \quad z = \infty \quad r \ge 0$$

$$C = C^b \quad z \ge 0 \quad r = \infty \tag{11}$$

has been solved by several authors[21] in different ways and is given by[27]

$$(\partial C/\partial z)_{z=0} = 2C^b/\pi[1/(a^2 - r^2)^{1/2}], \quad 0 \le r \le a \tag{12}$$

(27) Crank, J. *The Mathematics of Diffusion*, 2nd ed.; Clarendon Press: Oxford, 1975; p 43.

For the recessed disk-shaped electrode shown in Scheme 1, a simplified model with the following boundary conditions is proposed:

$$C = C^l \quad z = l \quad r \le a$$

$$\partial C/\partial z = 0 \quad z = l \quad r > a$$

$$C = C^b \quad z = \infty \quad r \ge 0$$

$$C = C^b \quad z \ge l \quad r = \infty \tag{13}$$

The concentration gradient at $z = l$ can be solved in a similar way and is given by

$$(\partial C/\partial z)_{z=l} = [2(C^b - C^l)/\pi][1/(a^2 - r^2)^{1/2}] \tag{14}$$

For simplicity, we have assumed that the concentration at $z = l$, C^l, is constant, independent of r. Thus, eq 2 derived here is only approximate. Equation 1 can be obtained by the following integration

$$i^0_{T,\infty} = \int_0^a nFD\left(\frac{\partial C}{\partial z}\right)_{z=0} 2\pi r dr \tag{15}$$

where the concentration gradient is given by eq 12.

Similarly, the steady-state current on a recessed disk electrode is obtained from the following integration with the concentration gradient given by eq 14.

$$i_{T,\infty} = \int_0^a nFD\left(\frac{\partial C}{\partial z}\right)_{z=1} 2\pi r dr$$

$$= 4nFD(C^b - C^l)a \tag{16}$$

For a cylindrical TLC with a base radius of a and a height equal to l, the steady-state diffusion current is given by

$$i_{TLC} = \pi a^2 nFDC^l/l \tag{17}$$

Here, we have assumed boundary conditions: $C = 0$ at $z = 0$ and $C = C^l$ at $z = l$.

From the requirement of current continuity, we have $i_{TLC} = i_{T,\infty}$. Thus,

$$C^l = 4lC^b/(4l + \pi a) \tag{18}$$

Substituting C^l of eq 18 into eq 17, we obtain

$$i_{TLC} = i_{T,\infty} = [\pi a/(4l + \pi a)](4nFDC^b a)$$

Thus,

$$i_{T,\infty} = [\pi a/(4l + \pi a)]i^0_{T,\infty} \tag{2}$$

Appendix B

Digital Simulation of Current at a Recessed Tip Approaching a Conductive Substrate. A finite difference method[28,29] was employed to simulate the observed response

(28) Bard, A. J.; Faulkner, L. R. *Electrochemical Methods: Fundamentals and Applications*; J. Wiley & Sons: New York, 1980; Chapters 3 and 4.

(29) Feldberg, S. W. In *Electroanalytical Chemistry*; Bard, A. J., Ed.; Marcel Dekker: New York, 1969; Vol. 3.

for cylindrical coordinates.

$$\partial C_i(r,z,t)/\partial t = D_i[\partial^2 C_i(r,z,t)/\partial r^2 + 1/r(\partial C_i(r,z,t)/\partial r) + \partial^2 C_i(r,z,t)/\partial z^2]$$

where C_i is the concentration of species i as a function of time, t, and coordinates r (radial) and z (normal). An exponentially increasing space grid[30,31] and the alternate-direction implicit method[31,32] was employed. Details of the simulation are given in supporting information.

Appendix C

Approximate Equation for Compression of Recessed Electrode against Substrate. We take the idealized geometry shown in Scheme 2 for the wax-sheathed metal tip and assume that the insulating wax flows inward and outward by equal amounts as it is compressed against the substrate. Thus,

$$[\pi(a_0^2 - a^2)\Delta l]/2 = \pi[a^2 - (a - \Delta a)^2](l - \Delta l)$$

$$(a - \Delta a)^2 = [2la^2 - \Delta l(a_0^2 + a^2)]/2(l - \Delta l) \quad (19)$$

From the steady-state TLC current and eq 19, we have

$$i_{TLC} = [\pi(a - \Delta a)^2 nFDC^b]/(l - \Delta l) \quad (31)$$

$$= \{\pi[2la^2 - \Delta l(a_0^2 + a^2)]/[8a(l - \Delta l)^2]\}4nFaDC^b$$

or

$$i_{TLC} = \{\pi[2la^2 - \Delta l(a_0^2 + a^2)]/[8a(l - \Delta l)^2]\}i^0_{T,\infty} \quad (3)$$

By defining several dimensionless variables $I \equiv i_{TLC}/i_{T,\infty}$, $L \equiv (l - \Delta l)/a$, $A_0 \equiv a_0/a$, $\Delta L \equiv \Delta l/a$, and $I^0 \equiv i^0_{T,\infty}/i_{T,\infty}$, we can write eq 3 in a normalized form

$$I = \{\pi[2L + \Delta L(1 - A_0^2)]/8L^2\}I^0 \quad (20)$$

Acknowledgment. The support of this research by the Laboratory of Electrochemistry and grants from the Robert A. Welch Foundation and the National Science Foundation (CHE-9508525) is gratefully acknowledged.

Supporting Information Available: Chronology of the single molecule electrochemistry experiments and details of the digital simulation of current at a recessed tip approaching a conductive substrate (15 pages). See any current masthead page for ordering and Internet access instructions.

JA9610794

(30) Feldberg, S. W. *J. Electroanal. Chem.* **1981**, *127*, 1.
(31) Kwak, J.; Bard, A. J. *Anal. Chem.* **1989**, *61*, 1221.
(32) Press, W. H.; Flannery, B. P.; Teukolsky, S. A.; Vetterling, W. T. *Numerical Recipes in C: The Art of Scientific Computing*; Cambridge University Press: Cambridge, 1988; pp 681−688.
(33) Unwin, P. R.; Bard, A. J. *J. Phys. Chem.* 1991, *95*, 7814.